

1  
2  
3  
4  
5  
6  
7  
8  
9  
10  
11  
12  
13  
14  
15  
16  
17  
18  
19  
20  
21  
22  
23  
24  
25

**Comparison and Distribution of Copper Oxide Nanoparticles and Copper Ions in  
Activated Sludge Reactors.**

DONGQING ZHANG<sup>1</sup>, ANTOINE P. TRZCINSKI<sup>2\*</sup>, HYUN-SUK OH<sup>3</sup>, EVELYN CHEW<sup>1</sup>,  
SOON KEAT TAN<sup>1</sup>, WUN JERN NG<sup>1</sup>, YU LIU<sup>1</sup>.

*<sup>1</sup>Advanced Environmental Biotechnology Centre, Nanyang Environment and Water Research  
Institute, 1 Cleantech loop, #06-10, Singapore 637141.*

*<sup>2</sup>School of Civil Engineering & Surveying, Faculty of Health, Engineering and Sciences,  
University of Southern Queensland, 4350 Australia.*

*<sup>3</sup>Singapore Membrane Technology Centre, Nanyang Environment and Water Research Institute,  
1 Cleantech loop, #06-10, Singapore 637141.*

---

\*Address correspondence to Dr Antoine TRZCINSKI, School of Civil Engineering & Surveying,  
Faculty of Health, Engineering and Sciences, University of Southern Queensland, 4350 Australia,  
Telephone number: +61 7 4631 1617;  
Email: [antoine.trzcinski@usq.edu.au](mailto:antoine.trzcinski@usq.edu.au),

## 26 **Abstract**

27

28 Copper oxide nanoparticles (CuO NPs) are increasingly applied in the industry which results  
29 inevitably in their release of these materials into the hydrosphere. In this study, simulated waste  
30 activated sludge experiments were conducted to investigate the effects of Copper Oxide NPs at  
31 concentrations of 0.1, 1, 10 and 50 mg/L and compare it with its ionic counterpart (as CuSO<sub>4</sub>). It  
32 was found that 0.1 mg/L CuO NPs had negligible effects on Chemical Oxygen Demand (COD)  
33 and ammonia removal. However, the presence of 1, 10 and 50 mg/L CuO NPs decreased COD  
34 removal from 78.7% to 77%, 52.1% and 39.2%, respectively ( $p < 0.05$ ). The corresponding  
35 effluent ammonium (NH<sub>4</sub>-N) concentration increased from 14.9 mg/L to 18, 25.1 and 30.8 mg/L,  
36 respectively. Under equal Cu concentration, copper ions were more toxic towards  
37 microorganisms compared to CuO NPs. CuO NPs were removed effectively (72-93.2%) from  
38 wastewater due to a greater biosorption capacity onto activated sludge, compared to the copper  
39 ions (55.1%-83.4%). The SEM images clearly showed the accumulation and adsorption of CuO  
40 NPs onto activated sludge. The decrease in Live/dead ratio after 5 h exposure of CuO NPs and  
41 Cu<sup>2+</sup> indicated the loss of cell viability in sludge flocs.

42

43 **Keywords:** CuO nanoparticles; copper ions; waste activated sludge; biosorption

44

## 45 **Introduction**

46

47 Nanotechnology has become very popular over the last few decades due to significant advances  
48 with applications in medicine and semiconductor, chemical and electronics industries. <sup>[1-3]</sup> As one  
49 of the most important engineered applications, copper oxide nanoparticles (CuO NPs) exhibit  
50 optical, electrical and catalytic properties, and have been used intensively in electronics,

51 ceramics, chemical sensors, polymers inks, metallic and coating. <sup>[4-6]</sup> Particularly, CuO NPs are  
52 commonly generated in large amounts during wafer chemomechanical polishing operations,  
53 which is a major source of wastewater in semiconductor manufacturing. <sup>[7]</sup> The increasing use of  
54 CuO NPs in industry and consumer products raises the concerns about the environmental risks  
55 due to their novel physical and chemical properties. Therefore, it is imperative to understand the  
56 environmental impact of CuO NPs.

57 Results from material flow analyses suggest that a major fraction of the NPs in commercial  
58 products will eventually enter municipal or industrial wastewaters, and subsequently reach  
59 wastewater treatment plants (WWTPs). <sup>[8, 9]</sup> WWTPs are considered as the last barriers prior to  
60 their environmental release. <sup>[10]</sup> Therefore, efficient removal of engineered NPs from wastewater  
61 is particularly important in view of their increasing evidence for their ecotoxicity. <sup>[11]</sup>

62 Furthermore, their toxicity to some microorganisms within the biological systems of WWTPs is  
63 of particular concern, since the inhibition and loss of certain bacterial species involved could be  
64 detrimental to biological treatment performance. <sup>[12]</sup> Previous study by Otero-González et al. <sup>[13]</sup>  
65 indicated that the extended exposure to even relatively low concentration (1.4 mg/L) of CuO NPs  
66 had a markedly negative effect on the performance of methanogenesis in upflow anaerobic  
67 sludge blanket (UASB) reactor. In another recently study, 50% inhibition of CH<sub>4</sub> production was  
68 also observed during anaerobic digestion processes in the presence of 11 mg Cu L<sup>-1</sup> of CuO NPs  
69 over a 14-d period. <sup>[14]</sup>

70 In addition, the fate, transport, and toxicity of NPs in wastewater treatment processes may differ  
71 largely from those of their ionic counterparts, due to the differences in the properties (size,  
72 charge density), chemical composition of media (pH, organics, ionic strength), test conditions,  
73 and organisms evaluated. <sup>[10]</sup> CuO NPs and Cu<sup>2+</sup> ions were reported to show different toxicity to  
74 some microbes. <sup>[15, 16]</sup> In a recent study of the toxic effects of CuO NPs, bulk CuO and CuSO<sub>4</sub> on  
75 *Tetrahymena thermophila*, Mortimer et al. <sup>[15]</sup> indicated that the most toxic Cu compound was

76 CuSO<sub>4</sub>, which was approximately 120 times more toxic than CuO NPs and 1500 times more  
77 toxic than bulk CuO. The different toxicity of Cu compounds has also been reported in a study of  
78 Heinlaan et al. <sup>[16]</sup> where the EC<sub>50</sub> values for bulk CuO, CuO NPs and CuSO<sub>4</sub> were 3811, 79, 1.6  
79 mg/L (*Vibrio fischer*); 165, 3.2, 0.17 mg/L (*Daphnia magna*); and 95, 2.1, 0.11 mg/L  
80 (*Thamncephalus platyurus*), respectively. However, Aruoja et al. <sup>[17]</sup> investigated the toxicities  
81 of ZnO, TiO<sub>2</sub> and CuO NPs to microalgae *Pseudokirchneriella subcapitata* and reported that the  
82 bioavailable EC<sub>50</sub> values of CuO NPs were not significantly different from the EC<sub>50</sub> of CuSO<sub>4</sub>  
83 (0.02 mg Cu/L).

84 There is a lack of information on the behaviour of CuO NPs in WWTPs and the effects of CuO  
85 NPs on the treatment performance in terms of organic removal and nitrification. <sup>[12, 13]</sup> In  
86 particular, a detailed evaluation of the extent to which CuO NPs were removed, characteristics of  
87 CuO NPs in suspension and/or sludge, and a comparison of the above with ionic salts, is  
88 currently not available. <sup>[10]</sup> Most authors have investigated specific microorganisms or activated  
89 sludge fed with synthetic wastewater. Studies with real wastewater are still scarce, but important  
90 because interactions with natural organic matter in real wastewater may result in different  
91 behaviour of CuO NPs. For instance, Cu ions can generate complex with humic acids due to their  
92 carboxylic and phenolic groups or precipitate as insoluble copper hydroxide.

93 Therefore, the objectives of this study were (a) to compare the short term effects and fate of CuO  
94 NPs and Cu<sup>2+</sup> in a laboratory scale waste activated sludge process fed with real wastewater; (b)  
95 to investigate the effects of 0.1, 1, 10 and 50 mg/L CuO NPs on COD and nitrogen removals; (c)  
96 to determine the accumulation of Cu ions in the effluent and onto activated sludge over short  
97 term experiments; (d) to determine the morphology of activated sludge using Scanning electron  
98 microscopy (SEM); (e) to assess the impacts of the presence of CuO NPs and Cu<sup>2+</sup> ions on  
99 bacterial integrity using the Live/Dead *Ba*clight bacterial viability technique which was not used

100 previously in particular under short term experiments (5 hours) at concentrations as high at 50  
101 mg/L.

102

## 103 **Materials and methods**

104

### 105 *Activated sludge and wastewater*

106

107 Primary wastewater was collected from Ulu Pandan Water Reclamation Plant (WRP), Singapore.  
108 The total treatment capacity of Ulu Pandan WRP is 361,000 m<sup>3</sup> per day. The treatment process  
109 includes typical preliminary, primary and secondary treatment processes. The wastewater was  
110 collected from the effluent of the primary sedimentation tank. As Ulu Pandan WRP treats  
111 combined industrial and domestic wastewater, the contaminant concentrations are expected to be  
112 higher than those in common domestic WWTPs. Real wastewater was stored at 4°C until it was  
113 fed to the SBRs.

114

### 115 *CuO NPs characterization*

116

117 The CuO NPs were purchased from Sigma-Aldrich (Singapore) with average particles size of  
118 40±5 nm. CuO NPs stock solutions (100 mg/L) were prepared by adding dry particles into Milli-  
119 Q (pH=6.8±0.2), and then the suspensions were sonicated (30°C, 100 W, 40 kHz) for 30 min and  
120 shaken for 2 h to increase their dispersion. *Zeta* potential of CuO NPs in the suspensions were  
121 measured using a Nanosizer (Malvern Instruments Ltd., UK). The morphology of the CuO NPs  
122 was examined using transmission electron microscopy (TEM) (JEOL JEM-3010, Japan). To  
123 avoid agglomeration or aggregation, water bath ultrasonic treatment was carried out to increase  
124 their dispersion before the use the suspension of CuO NPs.

125

126 *Sequencing batch reactors (SBR)*

127

128 SBRs were designed to simulate a full-scale operation of aeration and secondary clarification as  
129 described by Hou et al. [18] The SBRs (0.5 L) were seeded with return nitrifying activated sludge  
130 from Changi Water Reclamation Plant (Singapore) adjusted to a mixed liquor suspended solids  
131 (MLSS) concentration of 3 g/L. The hydraulic retention time (HRT) was 12 hours, while the  
132 sludge retention time (SRT) was 15 days. The steady state was established through monitoring  
133 the chemical oxygen demand (COD) and ammonium. The SBRs were operated under anoxic-  
134 aerobic conditions and each cycle had a duration of 8 h, including 1 h feeding, 1 h of anoxic  
135 period, 3 hours of aeration, settling for 2 h and effluent withdrawal for 1 h. After each cycle,  
136 supernatants following settling were replaced with primary clarifier effluent from Ulu Pandan  
137 Water Reclamation Plant to start the next cycle. The general parameters, such as pH, dissolved  
138 oxygen, and temperature were monitored and automatically recorded using a data logger. Both  
139 SBRs were run at a temperature of 24-26°C.

140 After 15 days of stabilisation period, four SBRs were spiked with CuO NPs at the concentrations  
141 of 0.1, 1, 10, and 50 mg CuO/L, respectively and three SBRs were spiked with corresponding  
142 ionic salt (in the form of CuSO<sub>4</sub>) at concentration of 0.2, 2.0, 20, and 100 mg/L CuSO<sub>4</sub>/L such  
143 that both sets of SBR contained exactly 0.08, 0.8, 8.0 and 40.0 mg Cu<sup>2+</sup>/L, respectively. One  
144 SBR was employed as control with no Copper addition. Each condition was operated for one  
145 month and steady state data were collected over three cycles to determine average and standard  
146 deviation.

147

148 *Analytical methods*

149

150 Sampling commenced after 15 days of operation of reactor, in order to ensure stable operation.  
151 Aliquots of completely mixed liquor suspensions were collected every 0.5 h over a period of 5 h.  
152 Collected samples were first centrifuged for 20 min at 10,000 rpm (Eppendorf 5810R). The  
153 measurement of MLSS, mixed liquor volatile suspended solids (MLVSS), chemical oxygen  
154 demand (COD), ammonium ( $\text{NH}_4^+\text{-N}$ ), and phosphate ( $\text{PO}_4^{3-}$ ) was in accordance with the  
155 Standard Methods. <sup>[19]</sup> All chemical tests were done in triplicate.  
156 The Cu levels in both liquid sample and biosolids were determined as described by microwave  
157 plasma – Atomic Emission Spectroscopy (MP-AES). <sup>[13]</sup> Briefly, 10 mL collected samples were  
158 first centrifuged for 10 min at 10,000 rpm prior to metal analysis (Eppendorf 5810R). Then the  
159 supernatant (2 mL) were collected and mixed with 2 mL of  $\text{HNO}_3$  (69%, Sigma-Aldrich) and  
160 shaken overnight at  $30\pm 2^\circ\text{C}$  to ensure complete Cu dissolution. Thereafter, Cu concentrations in  
161 liquid samples were determined by MP-AES (4100, Agilent Technologies) in triplicate. Cu level  
162 in biosolids was measured after digestion in an Anton Paar Microwave Reaction System  
163 (Multiwave 3000, Alpha Analytical USA) following EPA method 3051A. <sup>[13]</sup> All chemical tests  
164 were done at least in duplicates.

165

### 166 ***Bacterial viability assay***

167

168 The impact on bacteria integrity in the presence of CuO NPs and copper salt were assessed using  
169 a LIVE/DEAD *Ba*clight bacterial viability kit (Molecular Probes, USA). Viable and dead cells  
170 were detected by a green fluorescent nucleic acid stain, SYTO 9, which generally labels all  
171 bacteria (live and dead) with a green fluorescence, and a red fluorochrome, propidium iodide (PI),  
172 which stains only bacteria with damaged membranes due to its membrane impermeability. At the  
173 end of the experiment, 1 mL of the sludge suspension was stained with 1.5  $\mu\text{L}$  of SYTO9 and 1.5  
174  $\mu\text{L}$  of PI for 15 min in the dark at room temperature. The stained samples was covered with

175 cover slip and visualized using Nikon A1R confocal laser scanning microscope (CLSM) system  
176 attached to an upright ECLIPSE 90i machine with a 40× objective lens (Nikon, Tokyo, Japan).  
177 All images were acquired at a scale of 79.55 μm × 79.55 μm with 5.11 μm of confocal slice. The  
178 images were further analysed by Imaris software (Bitplane AG, Zurich, Switzerland) to calculate  
179 live/dead ratio.

180

### 181 *Scanning electron microscopy (SEM) and transmission electron microscope (TEM) imaging*

182

183 Samples were investigated using TEM and SEM. In the first case TEM grids were prepared by  
184 placing a drop of suspension (mixed liquor or supernatant) on a holey carbon grid and drawing  
185 the suspension through the TEM grid using a paper tissue. The TEM grids were washed  
186 afterwards in a drop of distilled water to remove the dissolved compounds. <sup>[20]</sup> The TEM was  
187 operated at 200 kV to detect and characterize aggregation state of NPs in the solution.

188 To prepare SEM image, mixed liquor was first washed 3 times with 0.1 M phosphate buffer  
189 solution (PBS) (pH 7.7) and fixed in 0.1 M phosphate buffer (7.4) containing 2.5%

190 glutaraldehyde at 4 °C for 4 h. The dried samples were coated with platinum before SEM

191 analysis according to Zheng et al. (2011). The elemental analysis of the particles was carried out  
192 using an energy-dispersive X-ray spectroscope (EDS).

193

### 194 *Statistical analysis*

195

196 The results are presented as average± standard deviation for each concentration. Tests to  
197 determine statistical differences between treatments were carried out by comparing the critical  
198 value through ANOVA one-way analysis of variance (SPSS Statistics V17.0). Comparisons were  
199 considered significantly different at  $p < 0.05$ .

200

## 201 **Results and discussion**

202

### 203 *Characterization of CuO NPs*

204

205 Figure 1 shows the TEM image of CuO NPs in deionized water under different magnifications  
206 (0.5  $\mu\text{m}$ , 100 nm and 50 nm). In the present study, due to their small size and huge surface area,  
207 NPs tend to aggregate or agglomerate in aqueous phase. Although the CuO NPs used in this  
208 study have a diameter size within the nanometer range, some aggregates of different sizes were  
209 formed in the solution where the particles were suspended, even after sonication. The *zeta*  
210 potential was -41.7 mV at pH= 6.8 and -35.6 mV at pH=6.4 at the beginning and end of the  
211 experiment, respectively.

212

### 213 *Removal of CuO NPs and copper ions*

214

215 The Cu levels in the biomass-free effluent spiked with CuO NPs and copper salt is shown in  
216 Figure 2A. After 5 h exposure, the concentrations of released soluble  $\text{Cu}^{2+}$  were 0.028, 0.204,  
217 1.02 and 2.81 mg/L at the initial CuO NP concentration of 0.1, 1.0, 10 and 50 mg/L, respectively.  
218 This finding indicates that the majority of the Cu in the influent was adsorbed onto settled  
219 biomass. At the CuO NP concentrations of 0.1 and 1.0 mg/L, both supernatant and effluent Cu  
220 content were consistently low. The higher concentrations of released  $\text{Cu}^{2+}$  observed at the initial  
221 CuO NP concentrations of 10 mg/L and 50 mg/L can be attributed to the increased sludge  
222 surface charge and the decreased hydrophobicity resulting in more  $\text{Cu}^{2+}$  ions released from CuO  
223 NPs. [21] Furthermore, the Cu concentrations in copper salt treatment were 3.2, 3.1, 4.9 and 5.9  
224 fold higher than in the corresponding CuO NPs treatment (Fig. 2B). Less  $\text{Cu}^{2+}$  was released from

225 NP possibly because humic acids are able to stabilize nanoparticles and retard dissolution rates.

226 [22]

227 Interestingly, CuO NPs were removed more efficiently than copper salt in this study with

228 removal efficiencies ranging from 72% to 93.2% for CuO NPs, while the values were 55.1% to

229 83.4% for Cu<sup>2+</sup> ions treatment, suggesting that large fraction of CuO NPs was removed from the

230 wastewater. These observations also support the hypothesis that the mechanisms governing the

231 removal of CuO NPs and ionic copper are different. As for copper salt, it is highly possible that

232 the majority of the added copper salt may quickly undergo a transformation due to their

233 dissolution followed by complexation or precipitation. [10, 23] Furthermore, depending on the

234 wastewater characteristics, copper can also be removed by coagulation or ion exchange in

235 wastewaters. [24, 25] In contrast, the attenuation of the CuO NP concentration in the liquid is most

236 likely due to aggregation, settling and biosorption onto the biomass. [12, 26, 27]

237

### 238 *Effect of CuO NPs and copper ions on COD removal*

239

240 Prior to addition of CuO NPs, the COD concentration in the effluent was around 130 mg/L

241 which corresponds to a COD removal efficiency of 78.7% (Fig. 3). The presence of CuO NPs,

242 however, influenced the COD removal efficiencies, which slightly decreased to 77% ( $p < 0.05$ ) at

243 CuO NP concentrations of 1 mg/L, respectively. The exposure to 10 and 50 mg/L CuO NPs

244 further decreased COD removal efficiencies to 52.1% and 39.2%, respectively. The lower COD

245 removals was due to the high toxicity of the released Cu<sup>2+</sup> ions from CuO NPs which inhibited

246 microorganisms. It can also be explained by the increased cell surface charge resulting in

247 reduced hydrophobicity and floc breakage as suggested by previous studies. [28, 29] Our finding

248 implies that 1 mg/L CuO NPs will cause some disturbance to the waste activated sludge process

249 which was not reported previously. This finding is in disagreement with Tan et al. [29] who

250 revealed that both short- and long term exposure of 1.0 mg/L of ZnO NPs did not significantly  
251 impact COD removal, despite the fact that ZnO NPs may exhibit more toxic effects on specific  
252 microorganisms than CuO NPs. Chen et al. [21] investigated the influence of Cu NPs on the  
253 physical-chemical properties of activated sludge, and indicated that lower Cu NPs concentrations  
254 (5 mg/L) did not affect the sludge properties, while higher Cu NPs concentrations (30-50 mg/L)  
255 may deteriorate the physical-chemical properties of activated sludge.

256 When CuSO<sub>4</sub> was used, the Cu<sup>+2</sup> concentration quickly increased to 4.1 mg/L after only 30  
257 minutes and gradually increased to 16.6 mg/L after 300 minutes, which resulted in a greater  
258 toxicity. In this study, in the presence of 20 and 100 mg/L copper sulphate, COD removals were  
259 44.8% and 7.3%, which were significantly ( $p < 0.05$ ) lower than those (52.1% and 39.2%) in the  
260 presence of CuO NPs, showing that copper salt exhibited more severe toxicity towards microbes  
261 than CuO NPs. Moreover, the MLSS concentration decreased markedly to 1.2 g/L with 100  
262 mg/L CuSO<sub>4</sub> (data not shown), showing that flocs were disrupted and cell lysis took place. From  
263 Figures 2 and 3, it is clear that CuO NPs is less toxic than CuSO<sub>4</sub> due to the fact that Cu ions  
264 from CuSO<sub>4</sub> dissolve more readily in water. These findings are consistent with Heinlaan et al. [16]  
265 who evaluated the eco-toxicity of ZnO NPs, CuO NPs and TiO<sub>2</sub> to bacteria and crustaceans, and  
266 reported that CuSO<sub>4</sub> was approximately 100-fold more toxic than nano CuO to *Vibrio fischer*  
267 with LC<sub>50</sub> value of 1.6 versus 79 mg/L, and 1000-fold more toxic than nano CuO to *Daphnia*  
268 *magna* (0.17 versus 164.8 mg/L) and *Thamncephalus platyurus* (0.11 versus 94.5 mg/L). In this  
269 study, after the addition of 50 mg/L CuO-NPs (equivalent to 40 mg/L Cu<sup>+2</sup>), the measured Zn<sup>2+</sup>  
270 concentration in the effluent progressively increased to only 2.8 mg/L after 5 hours, indicating a  
271 low dissolution potential of ZnO-NPs in the system, and that the most likely cause of inhibition  
272 was therefore the adsorption of CuO NP onto bacterial cells.

273

274 ***Effect of CuO NPs and copper ions on ammonium removal***

275

276 The effect of CuO NPs and copper ions on  $\text{NH}_4^+\text{-N}$  removal are shown in Figure 4. The  $\text{NH}_4^+\text{-N}$   
277 removal in the presence of 0.1 (64.1%) were relatively stable with increasing exposure time and  
278 not statistically different ( $p < 0.05$ ) from the negative control at (64.8%) over a period of 5 h  
279 exposure. However, when activated sludge was exposed to 1, 10 and 50 mg/L CuO NPs, the  
280 effluent  $\text{NH}_4^+\text{-N}$  significantly ( $p < 0.05$ ) increased from 14.9 mg/L (control) to 18 mg/L, 25.1  
281 mg/L and 30.8 mg/L, respectively, suggesting that CuO NPs at 1 mg/L could start causing some  
282 inhibition to ammonia oxidizing bacteria. At higher CuO NP concentration, the flocculating  
283 ability deteriorated due to the increased cell surface charge and the decreased hydrophobicity  
284 made the sludge flocs more dispersed, which further increased the toxicity of the CuO NPs by  
285 increasing the contact between CuO NPs and bacteria. [21] This finding also indicated that  
286 biosorption of CuO NPs onto activated sludge induced adverse effects on the diversity and  
287 activity of nitrifying microbial species. Additionally, in the present study, effluent ammonia  
288 concentration (20.7 mg/L, 29.3 mg/L and 35.2 mg/L, respectively) in the presence of  $\text{CuSO}_4$   
289 were higher than those in the presence of ZnO NPs (18 mg/L, 25.1 mg/L and 30.8 mg/L,  
290 respectively), implying that  $\text{Cu}^{2+}$  ions exhibited more severe toxicity to ammonia oxidizing  
291 bacteria than ZnO NPs.

292

### 293 *Accumulation of CuO NPs and copper ions onto activated sludge*

294

295 Activated sludge biomass from biological wastewater treatment processes is able to remove  
296 heavy metals from wastewater, and biosorption plays an important role in heavy metal recovery.  
297 [30, 31] CuO NPs and dissolved  $\text{Cu}^{2+}$  have been observed to bind on the surface of activated sludge.  
298 [32] Previous studies reported that biosorption of CuO NPs can take place in activated sludge  
299 treatment [12] and anaerobic sludge treatment exposed to synthetic wastewater. [13] Different

300 mechanisms of partitioning of NPs to biosolids have been identified including binding to  
301 extracellular polymers or cell surface, active cellular uptake, entrapment into flocs and diffusion  
302 into biofilms. [33] In the present study, a gradual increase in the  $\text{Cu}^{2+}$  concentrations in the  
303 biosolids was observed for both CuO NPs and copper salt treatment (Fig. 5). The copper  
304 concentrations were 2.12, 7.29, 11.1 and 29.31 mg/g MLSS at the CuO NP concentrations of 0.1,  
305 1.0, 10 and 50 mg/L after 5 h exposure, respectively, which was 1.58, 1.51, 1.10 and 1.68 fold  
306 more than in the  $\text{CuSO}_4$  treatment. At 50 mg/L exposure, a mass balance on Zn revealed that 98%  
307 of Cu from CuO NPs ended up in biosolids and 2% in the effluent. For  $\text{CuSO}_4$ , the mass balance  
308 was 86% onto biosolids and 14% in effluent. This finding suggests that CuO NPs have greater  
309 potential for adsorption onto biosolids compared to  $\text{Cu}^{2+}$  ions, due to its smaller particles size  
310 and larger surface area, and this biosorption capacity increased with the concentration of CuO  
311 NPs. Furthermore, the higher copper levels found in the biosolids were mainly attributed to CuO  
312 NPs, instead of the released  $\text{Cu}^{2+}$  from CuO NPs, given the fact that CuO NPs have much less  
313  $\text{Cu}^{2+}$  release capacity, compared to copper salt. This finding also reinforces the results of  
314 previous studies [11, 34] which indicated that the primary process of NP removal from wastewater  
315 is believed to be associated with biosorption onto biomass, although NPs may undergo  
316 transformation (e.g., dissolution of metal ions from metal-based NPs). In addition, these  
317 observations also support the hypothesis that different mechanisms might govern the removal of  
318 CuO NPs and  $\text{Cu}^{2+}$  ions from wastewater. As for CuO NPs, the attenuation of the CuO NP  
319 concentration in the solution phase is most likely due to precipitation of Cu species and CuO NP  
320 adsorption onto the biomass. In contrast, copper salt quickly undergo dissolution followed by  
321 complexation and precipitation.

322

323 The morphological changes in the activated sludge induced by the accumulated CuO NPs and  
324  $\text{Cu}^{2+}$  were observed by SEM (Fig. 6A-6C). After 5 h exposure, the SEM images clearly showed

325 the accumulation and adsorption of CuO NPs onto activated sludge. Such observation  
326 corroborates previous study assessing the effect of CuO NPs on physicochemical stability of  
327 activated sludge flocs. [12] SEM images revealed differences in damage extent between CuO NPs  
328 and copper salt. Although these damage extent cannot be accurately quantified based on our  
329 SEM analyses, the ionic copper appeared to have transformed to larger size aggregates during  
330 the experiment. The accumulation of CuO NPs and Cu<sup>2+</sup> on activated sludge was also confirmed  
331 using EDS profile analysis to confirm their Cu-based composition (Fig. 6D-6E). The EDS profile  
332 clearly demonstrates a Cu peak that is absent in the sample from the control reactor.

333

### 334 ***Bacterial viability assay***

335

336 Figure 7 displays the bacterial viability in the control and in the activated sludge exposed to CuO  
337 NPs and copper salt for 5 h. Compared to the control (Fig. 7A), the density of the dead cells  
338 increased after the exposure of the activated sludge to 50 mg/L of CuO NPs (Fig. 7B) or 100  
339 mg/L Cu<sup>2+</sup> ions (Fig. 7C), indicating a loss in the cell viability. The structure of the activated  
340 sludge became loose with numerous small aggregates of bacterial cells which may result in  
341 dispersed flocs. This can be due to the adsorption of NPs onto the sludge and inhibition of cell  
342 activity after exposure to 50 mg/L ZnO NPs. This was supported by the significant reduction in  
343 contaminant removal observed under the exposure to CuO NPs and copper ions at higher  
344 concentrations in this study. This finding was in agreement with previous studies [12, 21] which  
345 revealed that higher concentrations of CuO NPs exhibited inhibitory effects on the activity of  
346 activated sludge microorganisms. In addition, a decrease in the live/dead ratio was observed after  
347 5 h exposure to CuO NPs (2.14) and copper ions (2.08) at high concentration of 50 mg/L,  
348 although it was not significantly ( $p < 0.05$ ) different compared to the control (2.20).

349 It has been extensively reported that the toxicity of CuO NPs to activated sludge would be  
350 mainly due to the release of soluble  $\text{Cu}^{2+}$  ions, and the toxicity of  $\text{Cu}^{2+}$  ions to microorganisms is  
351 well documented. <sup>[35, 36]</sup> However, our work demonstrated that biosorption of CuO NP onto  
352 sludge played a major role in inhibiting bacterial activity and not copper ions dissolution in the  
353 bulk. In the present study, only 2.69 mg/L  $\text{Cu}^{2+}$  was released from CuO NPs which is unlikely to  
354 have caused severe inhibition. A release of 1.85 mg/L was observed by Hou et al. <sup>[12]</sup> when  
355 sludge flocs were exposed to CuO NPs at the same initial concentration (50 mg/L). This  
356 discrepancy might have been attributed to the size difference of investigated CuO NPs ( $40 \text{ nm} \pm$   
357  $5 \text{ nm}$  in the present study versus  $92 \pm 12 \text{ nm}$  in Hou et al. <sup>[12]</sup>), which in turn may lead to the  
358 different interaction between NPs and bacteria, as well as the toxicity induced by NPs. Previous  
359 studies have reported that CuO NPs could enhance the production of extracellular polymeric  
360 substances (EPS), <sup>[12]</sup> which could strongly interact with the polymer matrix to impede the access  
361 of pollutants to the bacterial cells and further increase the toxic resistance of the activated sludge  
362 by retarding the contact of the metal with the bacteria within bioflocks. <sup>[37]</sup> However, once the  
363 amount of released metal ions increased, the protective capacity of EPS to impede the access of  
364 the CuO NPs to the activated sludge was weakened, due to their loose structure under high  
365 toxicity condition. This explains the increased inhibition of CuO NPs to activated sludge at  
366 higher concentrations observed in the present study. The toxicity of CuO NPs exposed to  
367 bacteria can also be attributed to the changes of the sludge properties. <sup>[21]</sup> At low concentrations  
368 of NPs, the dissolved  $\text{Cu}^{2+}$  ions from CuO NPs could function as the bridges between the  
369 functional groups on the surface of bacteria and help to aggregate the microbes and promote the  
370 bio flocculation formation. However, under higher concentrations of CuO NPs, the increased cell  
371 surface charge weakened the strength between EPS and cations, resulting in the deterioration of  
372 the flocculating ability of activated sludge. Moreover, it has been proven that the toxicity of CuO

373 NPs could damage the cell membrane of bacteria (e.g., *Escherichia coli*), which would directly  
374 lead to the death of cell. [35, 38]

375

## 376 **Conclusions**

377

378 In this study, the fate and behaviour of CuO NPs and copper ions in the waste activated sludge  
379 process were investigated in SBR. The data indicate that the activated sludge process has the  
380 potential to remove CuO NPs from wastewater. CuO NPs were efficiently retained by activated  
381 sludge and CuO NPs were removed more effectively from the wastewater compared to copper  
382 ions. Additionally, CuO NPs exhibited greater biosorption capacity and stronger affinity to  
383 sewage sludge than copper salt. The short-term exposure to CuO NPs at 1 mg/L could cause  
384 some effects on COD and ammonia removal. The exposure to CuO NPs and Cu<sup>2+</sup> ions at higher  
385 concentrations of 10 mg/L and 50 mg/L caused significant inhibition in biological wastewater  
386 treatment. The results of bacterial integrity analysis imply that CuO NPs and copper salt at  
387 higher concentrations reduced the viability of bacteria in the biological treatment process.

388

## 389 **Acknowledgments**

390

391 The authors would like to express sincere thanks to the Singapore Economic Development Board  
392 and the Environment & Water Industry Programme.

393

## 394 **References**

395

- 396 [1] Kusic, H.; D. Leszczynska; N. Koprivanac; I. Peternel. Role of quantum dots  
397 nanoparticles in the chemical treatment of colored wastewater: Catalysts or additional pollutants.  
398 J. Environ. Sci., **2011**, 23(9), 1479-1485.
- 399 [2] Dasari, T.P.; K. Pathakoti; H.M. Hwang. Determination of the mechanism of  
400 photoinduced toxicity of selected metal oxide nanoparticles (ZnO, CuO, Co<sub>3</sub>O<sub>4</sub> and TiO<sub>2</sub>) to E.  
401 coli bacteria. J. Environ. Sci., **2013**, 25(5), 882-888.
- 402 [3] Gottschalk, F.; T. Sonderer; R.W. Scholz; B. Nowack. Modeled environmental  
403 concentrations of engineered nanomaterials (TiO<sub>2</sub>, ZnO, Ag, CNT, fullerenes) for different  
404 regions. Environ. Sci. and Technol., **2009**, 43(24), 9216-9222.
- 405 [4] Cioffi, N.; N. Ditaranto; L. Torsi; R.A. Picca; L. Sabbatini; A. Valentini; L. Novello; G.  
406 Tantillo; T. Bleve-Zacheo; P.G. Zambonin. Analytical characterization of bioactive  
407 fluoropolymer ultra-thin coatings modified by copper nanoparticles. Analytical and Bioanalytical  
408 Chemistry, **2005**, 381(3), 607-616.
- 409 [5] Chen, P.C.; G. Shen; C. Zhou. Chemical sensors and electronic noses based on 1-D metal  
410 oxide nanostructures. IEEE Transactions on Nanotechnology, **2008**, 7(6), 668-682.
- 411 [6] Ren, G.; D. Hu; E.W.C. Cheng; M.A. Vargas-Reus; P. Reip; R.P. Allaker.  
412 Characterisation of copper oxide nanoparticles for antimicrobial applications. Int. J. Antimicrob.  
413 Agents, **2009**, 33(6), 587-590.
- 414 [7] Huang, H.L.; H.P. Wang. Speciation of nano-copper collected in molecular sieves from  
415 chemical-mechanical planarization wastewater. J. Electron Spectros. and Related Phenomena,  
416 **2005**, 144-147, 307-309.
- 417 [8] Brar, S.K.; M. Verma; R.D. Tyagi; R.Y. Surampalli. Engineered nanoparticles in  
418 wastewater and wastewater sludge - Evidence and impacts. Waste Manag., **2010**, 30(3), 504-  
419 520.

- 420 [9] Boxall, A.B.A.; K. Tiede; Q. Chaudhry. Engineered nanomaterials in soils and water:  
421 How do they behave and could they pose a risk to human health? *Nanomedicine*, **2007**, 2(6),  
422 919-927.
- 423 [10] Ganesh, R.; J. Smeraldi; T. Hosseini; L. Khatib; B.H. Olson; D. Rosso. Evaluation of  
424 nanocopper removal and toxicity in municipal wastewaters. *Environ. Sci. and Technol.*, **2010**,  
425 44(20), 7808-7813.
- 426 [11] Limbach, L.K.; R. Bereiter; E. Müller; R. Krebs; R. Gälli; W.J. Stark. Removal of oxide  
427 nanoparticles in a model wastewater treatment plant: Influence of agglomeration and surfactants  
428 on clearing efficiency. *Environ. Sci. and Technol.*, **2008**, 42(15), 5828-5833.
- 429 [12] Hou, J.; L. Miao; C. Wang; P. Wang; Y. Ao; B. Lv. Effect of CuO nanoparticles on the  
430 production and composition of extracellular polymeric substances and physicochemical stability  
431 of activated sludge flocs. *Biores. Technol.*, **2015**, 176, 65-70.
- 432 [13] Otero-González, L.; J.A. Field; R. Sierra-Alvarez. Inhibition of anaerobic wastewater  
433 treatment after long-term exposure to low levels of CuO nanoparticles. *Wat. Res.*, **2014**, 58,  
434 160-168.
- 435 [14] Luna-delRisco, M.; K. Orupöld; H.C. Dubourguier. Particle-size effect of CuO and ZnO  
436 on biogas and methane production during anaerobic digestion. *J. Hazard. Mat.*, **2011**, 189(1-2),  
437 603-608.
- 438 [15] Mortimer, M.; K. Kasemets; A. Kahru. Toxicity of ZnO and CuO nanoparticles to  
439 ciliated protozoa *Tetrahymena thermophila*. *Toxicology*, **2010**, 269(2-3), 182-189.
- 440 [16] Heinlaan, M.; A. Ivask; I. Blinova; H.C. Dubourguier; A. Kahru. Toxicity of nanosized  
441 and bulk ZnO, CuO and TiO<sub>2</sub> to bacteria *Vibrio fischeri* and crustaceans *Daphnia magna* and  
442 *Thamnocephalus platyurus*. *Chemos.*, **2008**, 71(7), 1308-1316.

- 443 [17] Aruoja, V.; H.C. Dubourguier; K. Kasemets; A. Kahru. Toxicity of nanoparticles of CuO,  
444 ZnO and TiO<sub>2</sub> to microalgae *Pseudokirchneriella subcapitata*. *Sci. Total Environ.* , **2009**, *407*,  
445 1461-1468.
- 446 [18] Hou, L.; K. Li; Y. Ding; Y. Li; J. Chen; X. Wu; X. Li. Removal of silver nanoparticles in  
447 simulated wastewater treatment processes and its impact on COD and NH<sub>4</sub> reduction. *Chemos.*,  
448 **2012**, *87*(3), 248-252.
- 449 [19] APHA, In *Standard Methods for the Examination of Water and Wastewater 22th edition*.  
450 Washington, D.C: 2012.
- 451 [20] Kaegi, R.; A. Voegelin; C. Ort; B. Sinnet; B. Thalmann; J. Krismer; H. Hagendorfer; M.  
452 Elumelu; E. Mueller. Fate and transformation of silver nanoparticles in urban wastewater  
453 systems. *Wat. Res.*, **2013**, *47*(12), 3866-3877.
- 454 [21] Chen, H.; X. Zheng; Y. Chen; M. Li; K. Liu; X. Li. Influence of copper nanoparticles on  
455 the physical-chemical properties of activated sludge. *PLoS ONE*, **2014**, *9*(3).
- 456 [22] Chaúque, E.F.C.; J.N. Zvimba; J.C. Ngila; N. Musee. Stability studies of commercial  
457 ZnO engineered nanoparticles in domestic wastewater. *Physics and Chemistry of the Earth, Parts*  
458 *A/B/C*, **2014**, *67-69*, 140-144.
- 459 [23] Hsu, H.F.; M. Kumar; Y.S. Ma; J.G. Lin. Extent of precipitation and sorption during  
460 copper removal from synthetic wastewater in the presence of sulfate-reducing bacteria. *Environ.*  
461 *Eng. Sci.*, **2009**, *26*(6), 1087-1096.
- 462 [24] Vreysen, S.; A. Maes; H. Wullaert. Removal of organotin compounds, Cu and Zn from  
463 shipyard wastewaters by adsorption - flocculation: A technical and economical analysis. *Marine*  
464 *Poll. Bull.*, **2008**, *56*(1), 106-115.
- 465 [25] Dobrevsky, I.; M. Dimova-Todorova; T. Panayotova. Electroplating rinse waste water  
466 treatment by ion exchange. *Desalination*, **1997**, *108*(1-3), 277-280.

- 467 [26] Bondarenko, O.; K. Juganson; A. Ivask; K. Kasemets; M. Mortimer; A. Kahru. Toxicity  
468 of Ag, CuO and ZnO nanoparticles to selected environmentally relevant test organisms and  
469 mammalian cells in vitro: A critical review. *Archives of Toxicology*, **2013**, *87*(7), 1181-1200.
- 470 [27] Karri, S.; R. Sierra-Alvarez; J.A. Field. Toxicity of copper to acetoclastic and  
471 hydrogenotrophic activities of methanogens and sulfate reducers in anaerobic sludge. *Chemos.*,  
472 **2006**, *62*(1), 121-127.
- 473 [28] Chen, Z.; Y. Wang; K. Li; H. Zhou. Effects of increasing organic loading rate on  
474 performance and microbial community shift of an up-flow anaerobic sludge blanket reactor  
475 treating diluted pharmaceutical wastewater. *J. Biosci. and Bioeng.*, **2014**.
- 476 [29] Tan, M.; G. Qiu; Y.P. Ting. Effects of ZnO nanoparticles on wastewater treatment and  
477 their removal behavior in a membrane bioreactor. *Biores. Technol.*, **2015**, *185*, 125-133.
- 478 [30] Fan, T.; Y. Liu; B. Feng; G. Zeng; C. Yang; M. Zhou; H. Zhou; Z. Tan; X. Wang.  
479 Biosorption of cadmium(II), zinc(II) and lead(II) by *Penicillium simplicissimum*: Isotherms,  
480 kinetics and thermodynamics. *J. Hazard. Mat.*, **2008**, *160*(2-3), 655-661.
- 481 [31] Göksungur, Y.; S. Üren; U. Güvenç. Biosorption of cadmium and lead ions by ethanol  
482 treated waste baker's yeast biomass. *Biores. Technol.*, **2005**, *96*(1), 103-109.
- 483 [32] Sheng, G.P.; J. Xu; H.W. Luo; W.W. Li; W.H. Li; H.Q. Yu; Z. Xie; S.Q. Wei; F.C. Hu.  
484 Thermodynamic analysis on the binding of heavy metals onto extracellular polymeric substances  
485 (EPS) of activated sludge. *Wat. Res.*, **2013**, *47*(2), 607-614.
- 486 [33] Westerhoff, P.K.; A. Kiser; K. Hristovski. Nanomaterial removal and transformation  
487 during biological wastewater treatment. *Environ. Eng. Sci.*, **2013**, *30*(3), 109-117.
- 488 [34] Kaegi, R.; A. Voegelin; B. Sinnet; S. Zuleeg; H. Hagendorfer; M. Burkhardt; H. Siegrist.  
489 Behavior of Metallic Silver Nanoparticles in a Pilot Wastewater Treatment Plant. *Environ. Sci.*  
490 *& Technol.*, **2011**, *45*(9), 3902-3908.

- 491 [35] Zhao, J.; Z. Wang; Y. Dai; B. Xing. Mitigation of CuO nanoparticle-induced bacterial  
492 membrane damage by dissolved organic matter. *Wat. Res.*, **2013**, *47*(12), 4169-4178.
- 493 [36] Gunawan, C.; W.Y. Teoh; C.P. Marquis; R. Amal. Cytotoxic origin of copper(II) oxide  
494 nanoparticles: Comparative studies with micron-sized particles, leachate, and metal salts. *ACS*  
495 *Nano*, **2011**, *5*(9), 7214-7225.
- 496 [37] Ma, J.; X. Quan; X. Si; Y. Wu. Responses of anaerobic granule and flocculent sludge to  
497 ceria nanoparticles and toxic mechanisms. *Biores. Technol.*, **2013**, *149*, 346-352.
- 498 [38] Duan, J.; Y. Yu; Y. Li; Y. Yu; Y. Li; X. Zhou; P. Huang; Z. Sun. Toxic Effect of Silica  
499 Nanoparticles on Endothelial Cells through DNA Damage Response via Chk1-Dependent G2/M  
500 Checkpoint. *PLoS ONE*, **2013**, *8*(4).

501

502

503 **FIGURE CAPTIONS**

504

505 **Figure 1.** CuO NPs (A-C) in deionized water at different resolution (i.e., 500, 100 and 50 nm)  
506 characterized by TEM. These are representative images of particles after drying the suspension on  
507 the microscope grid which resulted in aggregation.

508

509 **Figure 2.** Kinetics of Cu<sup>2+</sup> released from CuO NPs (A) and Cu<sup>2+</sup> released from CuSO<sub>4</sub> (B). Error  
510 bars represent standard deviations of triplicate measurements.

511

512 **Figure 3.** COD concentrations in the effluent of A) CuO NPs treatment; and B) CuSO<sub>4</sub> treatment.  
513 Error bars represent standard deviations of triplicate measurements.

514

515 **Figure 4.** NH<sub>4</sub>-N concentrations in the effluent of A) CuO NP treatment; and B) CuSO<sub>4</sub>  
516 treatment. Error bars represent standard deviations of triplicate measurements.

517

518 **Figure 5.** Cu<sup>2+</sup> concentrations in the biosolids for A) CuO treatment; and B) CuSO<sub>4</sub> treatment.  
519 Error bars represent standard deviations of triplicate measurements.

520

521 **Figure 6.** SEM images of activated sludge after CuO NPs and Cu<sup>2+</sup> ions exposure at the  
522 concentration of 10 mg/L after 5 h. A) Sludge in the control; B) Sludge in the treatment exposed  
523 to CuO NPs; and C) Sludge in the treatment exposed to Cu<sup>2+</sup> ions; D) EDS spectra for A); E)  
524 EDS spectra for B); and F) EDS spectra for C).

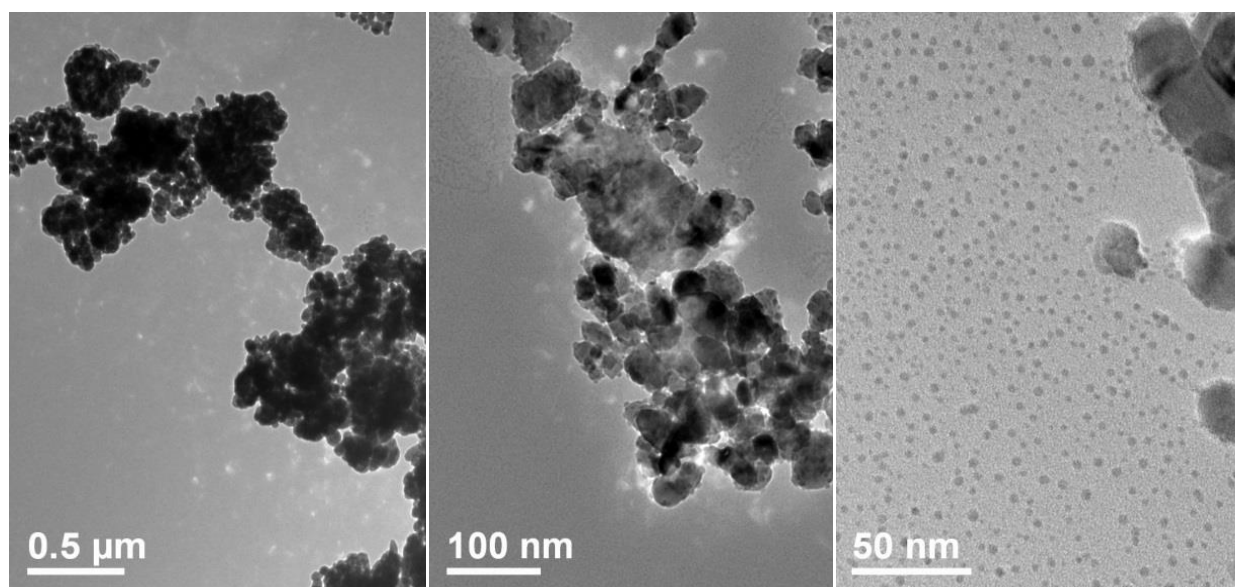
525

526 **Figure 7.** Bacterial viability in A) control treatment; B) in activated sludge exposed to CuO NPs  
527 at the concentration of 50 mg L<sup>-1</sup>; and C) in activated sludge exposed to CuSO<sub>4</sub> treatment at the  
528 concentration of 100 mg L<sup>-1</sup> at the end of the experiment using confocal microscopy.

529

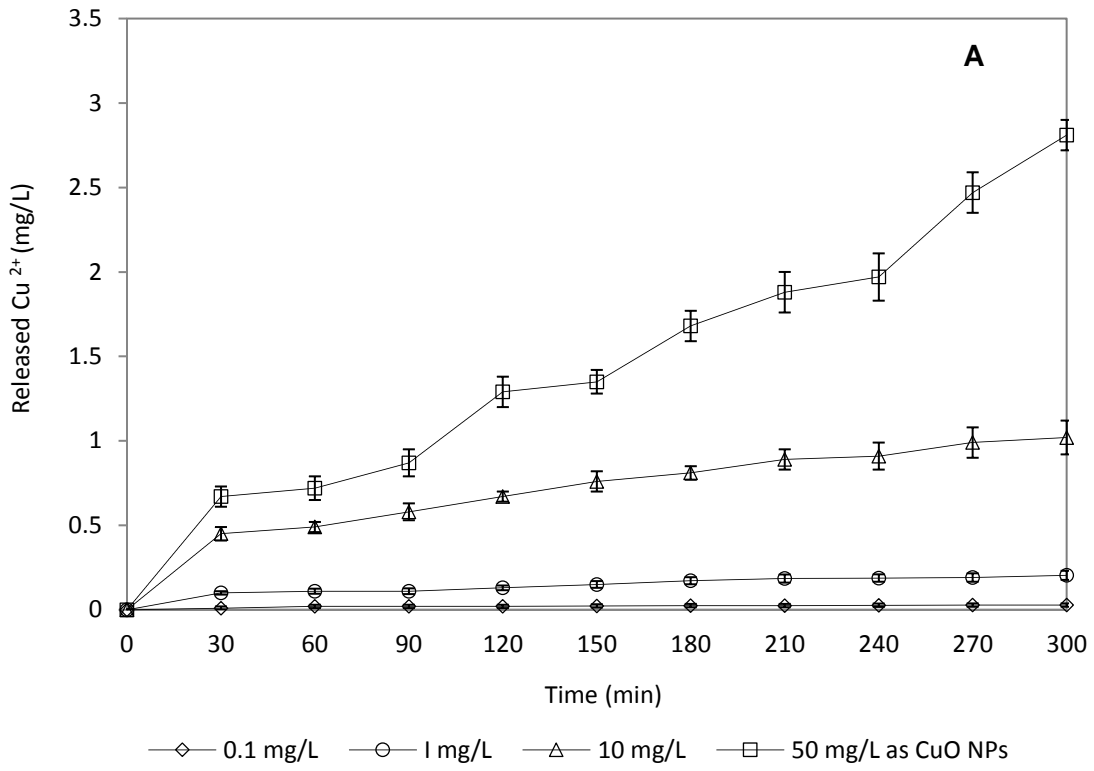
530

531



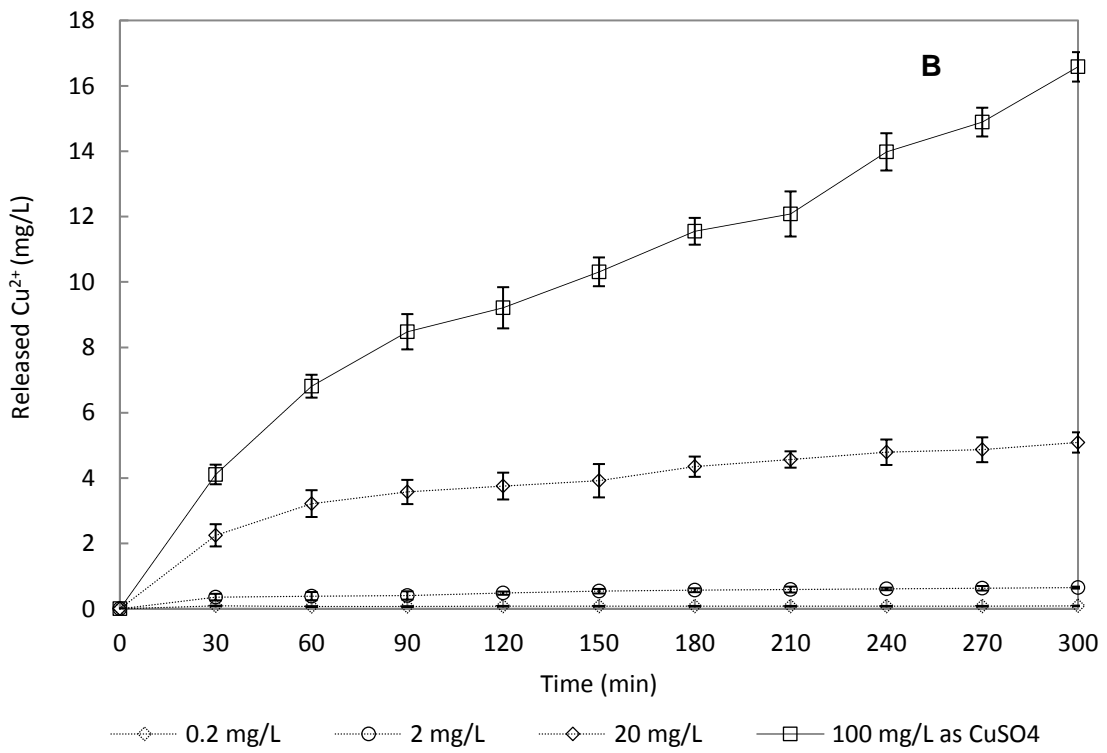
532

533 Fig. 1



534

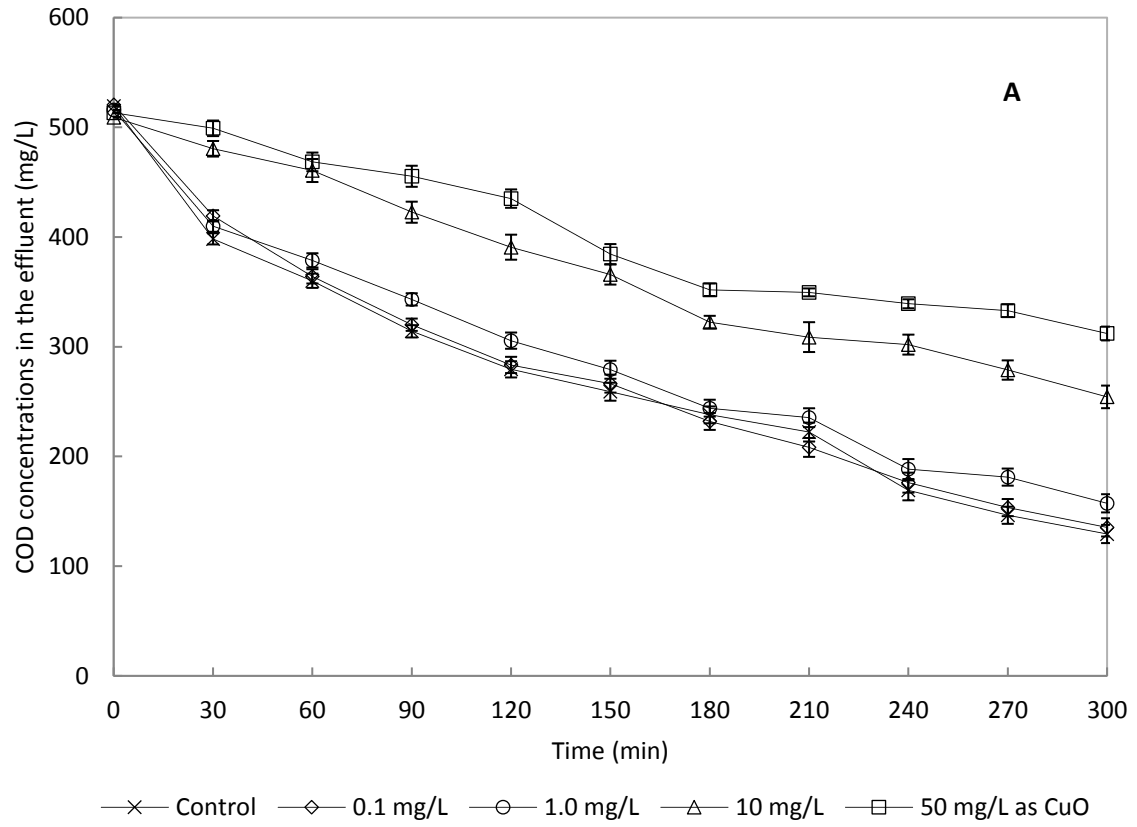
535



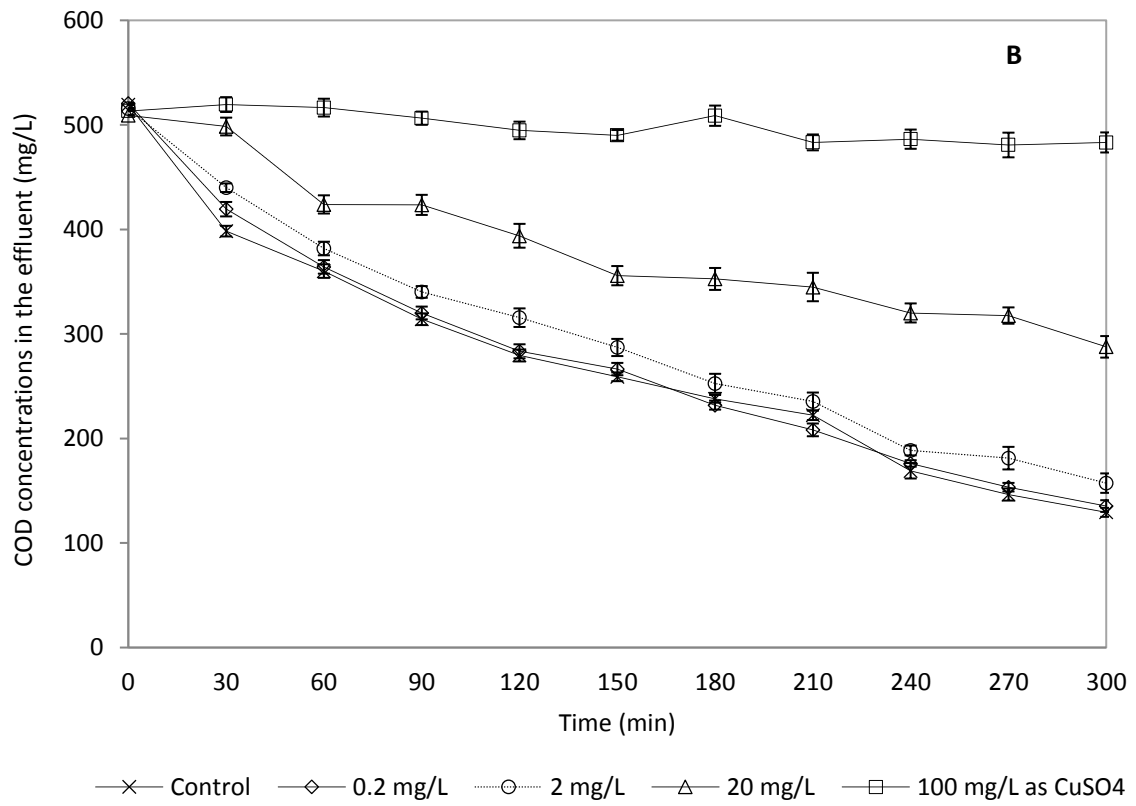
536

537 Fig. 2

538



539

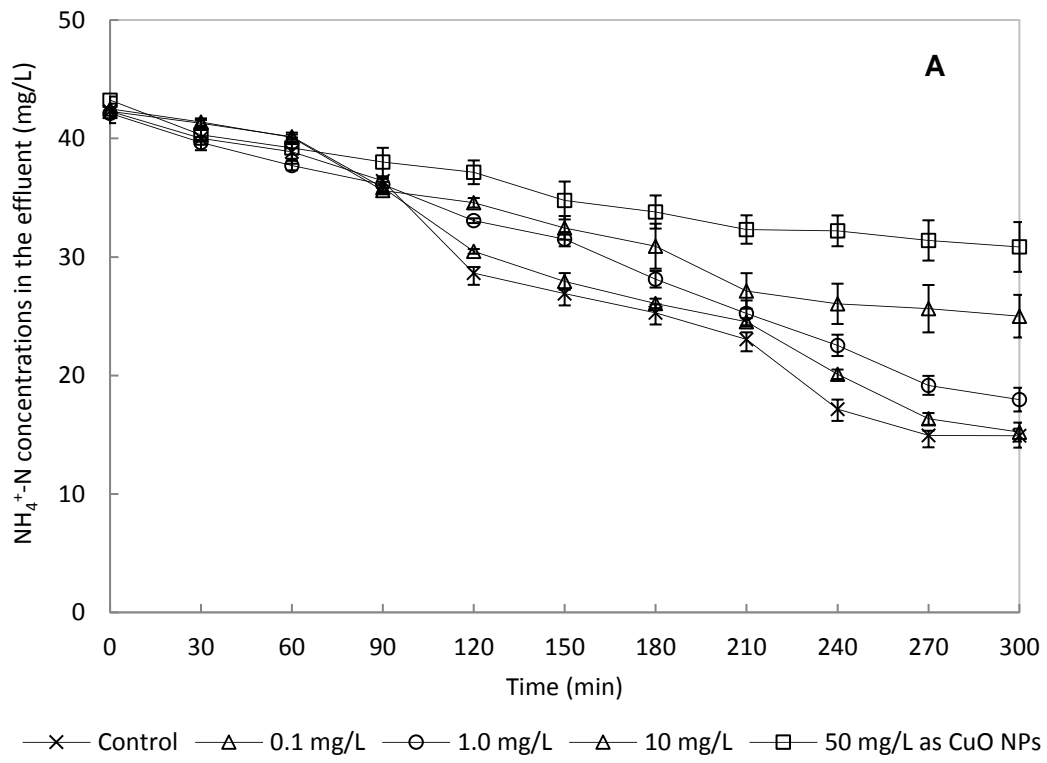


540

541

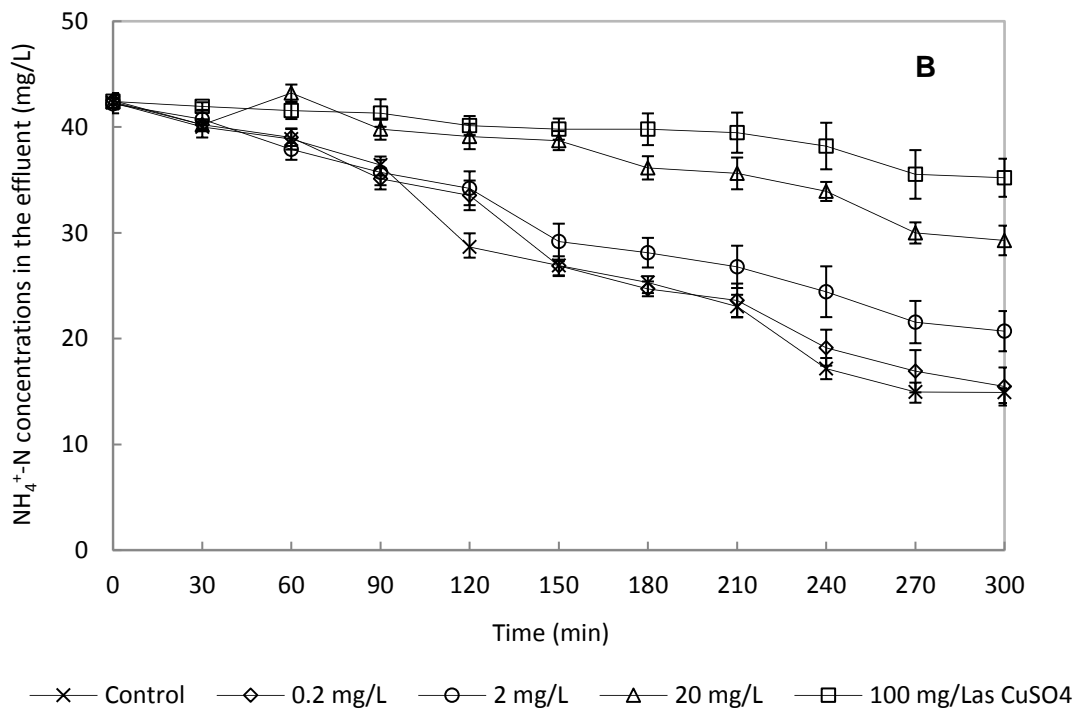
Fig. 3

542



543

544

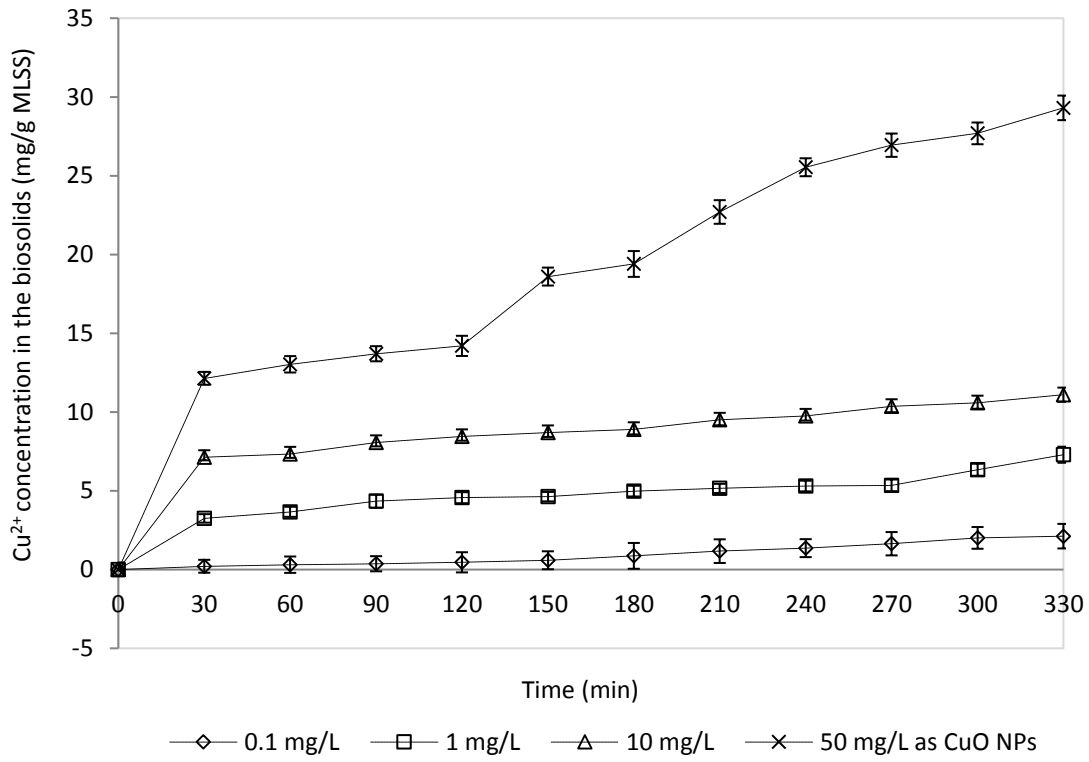


545

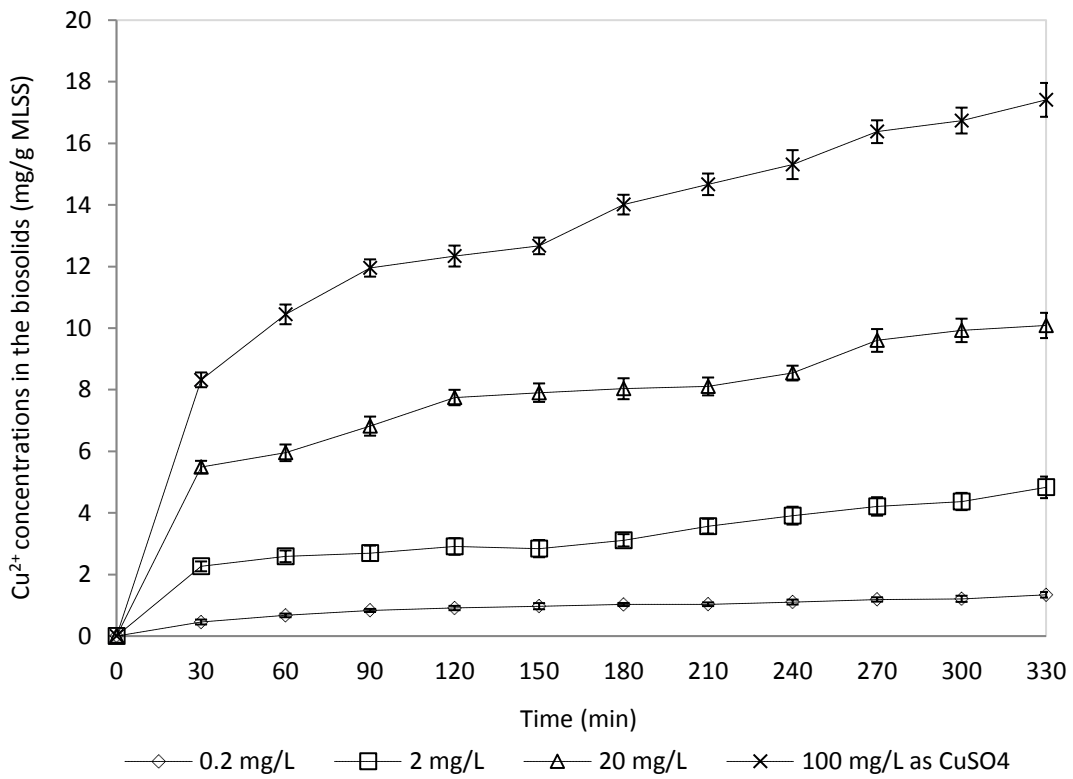
546

Fig. 4

547



548



549

550

Fig. 5

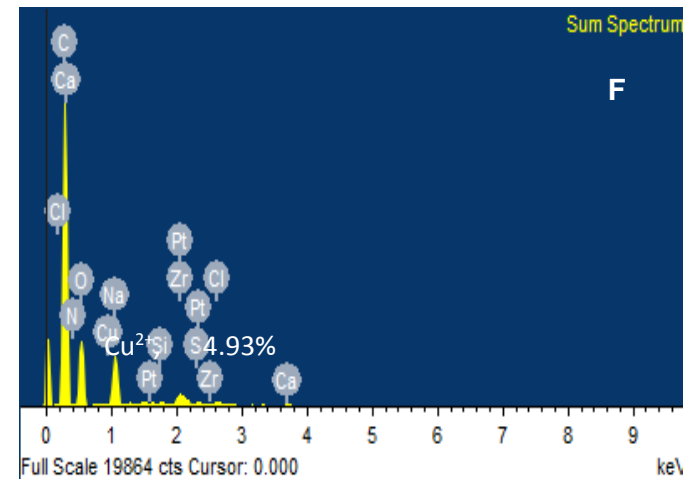
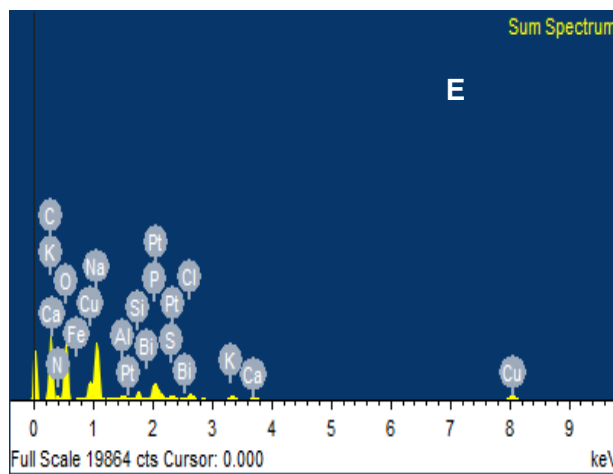
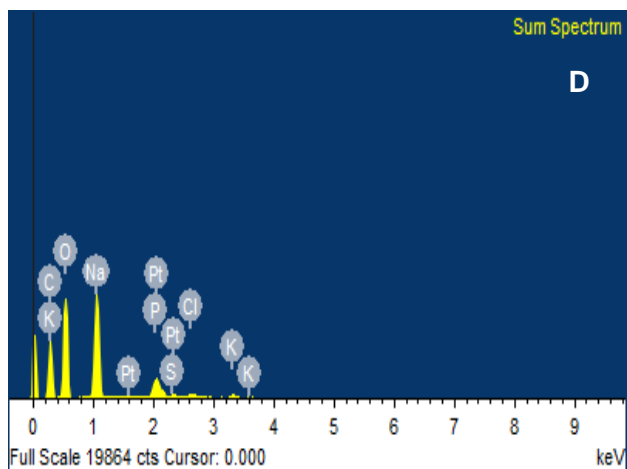
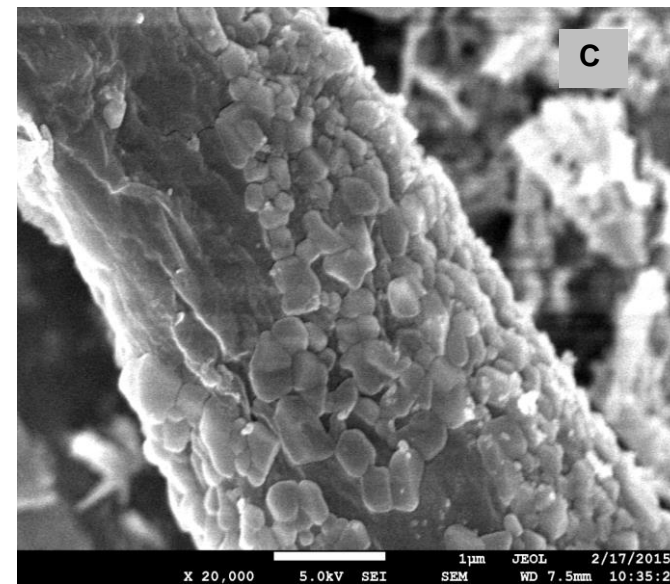
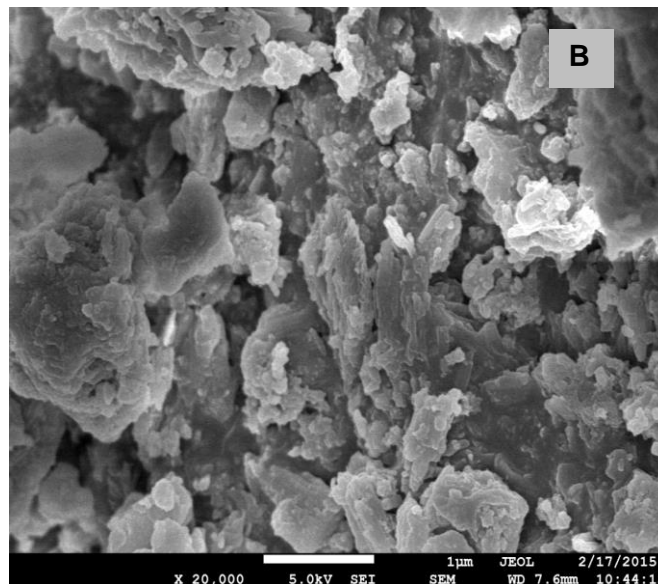
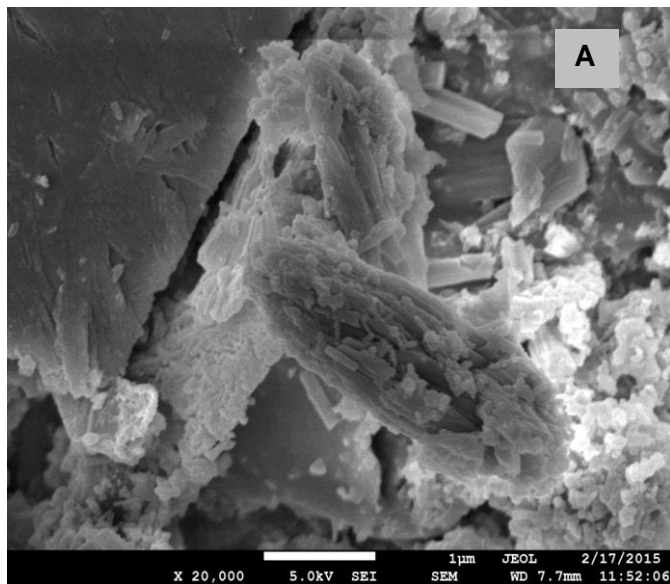
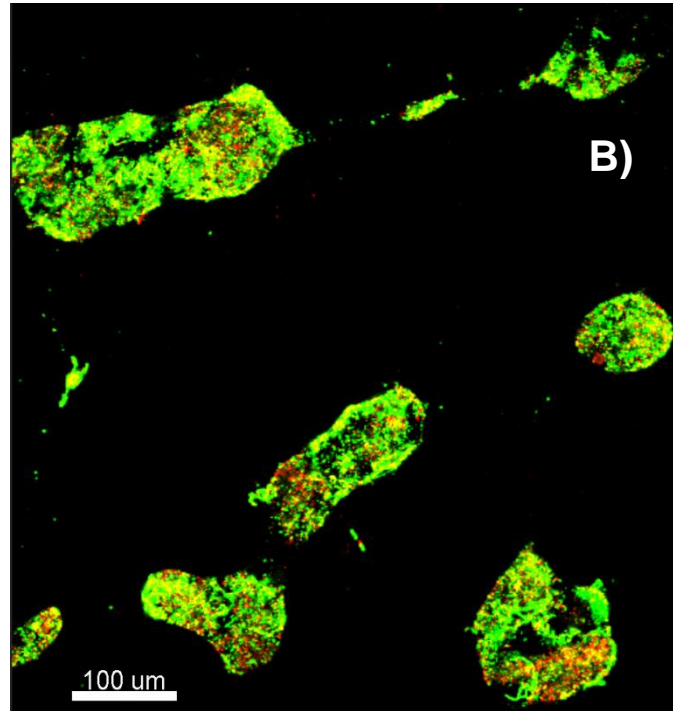
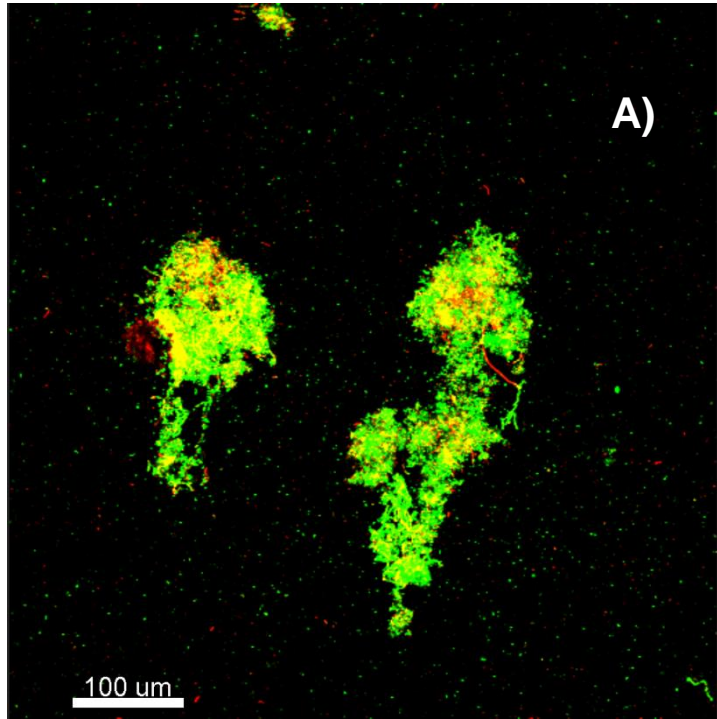
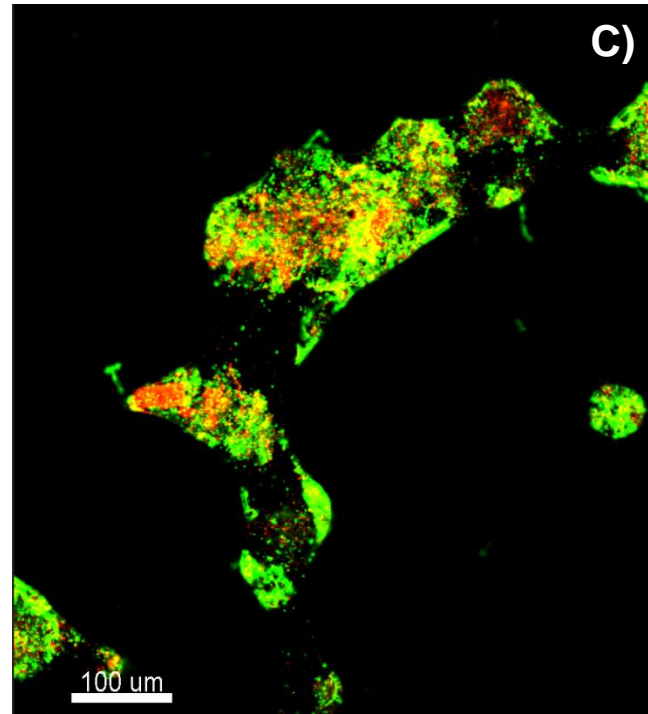


Fig. 6





551

552 Fig. 7

553